doi.org/10.26398/IJAS.0033-002

A SOLDERING RELIABILITY STUDY: A COMPARISON AMONG ALLOY-SURFACE FINISH COMBINATIONS CONSIDERING DIFFERENT COMPONENT PACKAGING

Rossella Berni[1]

Department of Statistics Computer Science Applications "G. Parenti", University of Florence, Italy

Marcantonio Catelani

Information Engineering Department, University of Florence, Italy

Caterina Fiesoli

Via di Cafaggiolo 54, 50060 Pelago, Florence, Italy

Valeria Leonarda Scarano

Via Pier Vettori 33, 00151 Rome, Italy

Abstract *The assembly process of components in a Printed Circuit Board (PCB) requires exposed copper areas coated with a surface finish. In the past, the predominant surface finish in the PCB industry was traditionally Hot Air Solder Leveling (HASL) combined with tin-lead as the soldering alloy. Besides replacing the soldering paste containing lead, the PCB industry has also been active in seeking surface finish options as an alternative to HASL. This research proposes a detailed and comparative study on the reliability behavior of a solder joint by considering different surface finishes and several component packages. In particular, different combinations of alloys (e.g. tin-lead, tin silver-copper) and surface finishes (e.g. HASL; Electroless Nickel Immersion Gold known - ENIG; Immersion Tin I-Sn; Organic Solderability Preservative - OSP), considering four types of components, were evaluated through Weibull distributed data and statistical models for reliability, with the aim to appraise how the type of package, or geometry of the joint are able to affect the soldering reliability. Two-by-two comparisons of alloy-surface finishes were carried out and the statistical results were presented. The tin-silver-copper alloy, with related finishes, reveals higher reliability than the boards soldered with the traditional alloy-finish combination.*

Keywords: *Reliability test, lead-free, soldering alloy, surface finish, Weibull statistical models.*

---

[1] Corresponding author: Rossella Berni, emal: rossella.berni@unifi.it

1. INTRODUCTION

In the last years, new and interesting materials have been introduced in the soldering process of PCB to address the reduction of the environmental pollution generated by the disposal of electronic devices traditionally soldered with Pb-Sn. The performance and reliability of the solder joint depend on the bulk properties of the structures (the solder, base materials, coatings, and surface finishes) and the interfaces between them, Vianco (2019). In 2012 a survey conducted by IPC and NPL (National Physical Laboratory) showed that surface finish solderability is the single most contributor to PCB defects, Puthota (2021). Therefore, when developing a new lead-free solder, the effects of different surface finishes should be considered and tested to evaluate the solderability of the new lead-free solder and the reliability of the solder joint. To this end, accelerated life tests, which are usually efficient for these purposes, were planned and implemented in our research, Catelani et al. (2013). It is important to underscore how solder joint reliability is one of the most critical design aspects of electronic assemblies, and it was analyzed in particular with the introduction of lead-free soldering technology, Lau (1991), Lau and Pao (1997), and Clech (2007). In previous studies, thermal and mechanical stress conditions were studied in order to evaluate creep, fatigue and fracture of lead-free alloy compositions, with silver (Ag) and copper (Cu) contents, Shangguan (2006), Suganuma (2001), and IPC-SM-785 (1992).

This paper focuses on the comparison of the most popular lead-free alloys, e.g. tin-silver-copper (known as SAC) with the traditional alloy (Sn-Pb), taking into account, as an important focal point, the board surface finishes in order to evaluate the reliability issues of soldering depending on different types of component package. The surface finish generates a critical interface between the solder and PCB pad. In the last years, the effect of surface finishes on the wettability, solder strength, and solder joint reliability have received an attention point in the PCB assembly process. Many researchers have reported the impacts of different surface finishes, e.g. Cu organic solderability preservatives (Cu−OSP), electroless nickel immersion gold (ENIG), and electroless nickel electroless palladium immersion gold (ENEPIG), on wettability and mechanical properties, ball pull strength, thermal cycle reliability, drop reliability, and electromigration reliability of solder joints formed by various solder alloys (e.g. SAC105, SAC205, SAC305, SAC405,SN100C, SACm, and SnBi−based solders), Shunfeng et al. (2017) and Sinan et al. (2019).

In particular, the SAC degradation studies based on finite element analyses, Cuddalorepatta and Dasgupta (2007) and Vasudevan and Fan (2008), demon-

strated high creep resistance. In addition to the finite element analysis, the greater reliability of the SAC compared to the Sn-Pb has also been experimentally confirmed in several studies, where lifetime data from accelerated life tests, mechanical or thermal, are considered, see among the others Osterman and Dasgupta (2007), Dudek et al. (2008), Andersson et al. (2004), and Kim et al. (2002). In Hossain et al. (2006) the impact of surface finishes was presented for a SAC soldering, but only for one type of package and mechanical loading as stress. In Zhang et al. (2008) and Ma et al. (2007) the authors addressed the SAC reliability by considering the importance of surface finish and package, but still only for one type of finish and one type of package. Reliability studies regarding the package geometry also connected to the miniaturization of systems were implemented in Yu et al. (2012). Moreover, in literature, great attention was often reserved to the soldering material on the package type with little, or no interest, in the surface finish. However, it is important to reflect on the reaction of the interface between the solder joints and the surface finishes, as demonstrated in Liu et al. (2015). Although many research studies have been conducted on lead free soldering SAC reliability, and the interfacial diffusion between SAC solder alloy and ENIG substrate, there is a gap in the literature regarding reliability performance of solder joints considering concurrently different surface finishes and component packages, Cheng et al. (2004), Islam and Chan (2005), Sun et al. (2006), Zribi et al. (2001), and Kim et al. (2004). In our research, the samples are aged for several designated time spans. In general, by considering empirical evidence emerging from experimental data related to any lifetime test, the application of statistical models for reliability seems to be the right choice for better improving and predicting the life expectancy. In particular, the structure of the data relating to the statistical modeling approach implies the consideration of the Weibull models for analysing data, e.g. resistance measurements, which were collected during thermal accelerated life tests. In the previous study, Berni et al. (2016), three two-by-two comparisons were carried out: i) the traditional SnPb-HASL combination versus SAC305-ENIG; ii) the SnPb-HASL combination versus SAC305-I-Sn; iii) the last comparison relates to SAC305-ENIG versus SAC305-I-Sn. The SAC305, including both ENIG and I-Sn finishes, demonstrated a higher reliability performance with respect to the boards soldered with the traditional combination, SnPb-HASL. These results are also confirmed by considering the most recent studies on long-term reliability of lead-free solder on three commonly used lead-free surface finishes with ceramic chip resistor, Collins et al. (2012), and the effect of different PCB surface finishes (OSP and ENIG) on the reliability performance of

SAC305 solder joints, investigated in Xia and Xie (2008), in which the results showed that OSP finishes outperformed ENIG finishes with cracks occurring earlier in the ENIG samples. In this paper, following the same line of reasoning as for Berni et al. (2016), a new combination of soldering-surface finish has been introduced (SAC305-OSP) and compared two-by-two with SnPb-HASL, SAC305-ENIG SAC305-I-Sn.

This paper is organized as follows. The next section describes the testing and the data, the statistical theory relating to the modeling approach is reported in the third section, the fourth section illustrates the model results, with discussion and final remarks at the end.

2. RELIABILITY TESTS AND DATA DESCRIPTION

In order to study the performance of solder alloys subject to thermal aging, the influence of surface finishes of the PCBs and different geometries of components soldered on PCBs were considered in this research.

The alloys Eutectic Sn-Pb, and SAC305As were studied. The Sn-Pb alloy, in particular with a eutectic composition of 63% Sn and 37% Pb, was the only alloy used for brazing and joining the electronic components to printed circuit boards for a long time. Among the various positive characteristics associated with this alloy, one of the greatest is the advantage of offering a melting temperature equal to $183°C$, which allowed for reducing the thermal energy supplied during the soldering process. Several alloys were also developed to substitute the tin-lead solder alloy, Bradley et al. (2007). The choice of alloys was based on the following considerations: toxicity level, physical properties, mechanical properties and microstructure, electrochemical properties, manufacturability, costs, and availability of materials. To date, the industry seems to tend to the ternary near-eutectic SAC, IPC/JEDEC J-STD-020C (2004), despite the increase in the melting temperature, higher than $30°C \sim 40°C$ compared to Sn-Pb solder alloys. Printed circuit boards requiring component attachment must have the exposed copper surface coated with a protective finish. This protective coating must be weldable, and at the same time, act as a barrier for preventing the copper from oxidizing which causes assembly problems for the end-user, AIM (2007).

Among the different surface finish processes for printed circuit boards, we considered OSP in comparison with HASL, ENIG and I-Sn.

OSP, also known as anti-tarnish material, on bare copper printed circuit boards is becoming more prevalent in the electronics industry as a low-cost replacement to the HASL. The OSP process is environment-friendly, provides a surface pla-

narity equivalent to the plated copper finish, and requires very low equipment maintenance. The use of OSP appears to be the only viable non-metallic surface finish option nowadays available. The OSP technology might be able to meet the technical requirements of the industry, since it costs less and eliminates lead for the PCBs manufacturer; it also demonstrates a high reliability performance. Even though HASL and ENIG finishes have wide applications, the first finish showed concerns relating to the development of whiskers, and the second one showed insidious problems with oxidation of nickel. The Tin immersion seems to be immune to whiskers, having a low temperature process with ease of operability; moreover, it also showed some problematic issues, in particular related to solderability and storage life, IPC-D-279 (1996).

In this study the HASL was adopted as a surface finish for Sn-Pb, with three board finishes, e.g. OSP, ENIG and I-Sn, using SAC305.

Furthermore, to evaluate whether, and how, the package type or the geometry of the joint affects the soldering reliability, together with the solder alloy and the surface finish of the board, four types of components were assembled on the boards under test. More specifically, these components refer to surface mount technology (SMT) with a plastic package; in particular:

- *TypeI*: components without a pin out of the package;
- *TypeII*: components with ball grid arrays;
- *TypeIII*: surface mount technology components with gull wing leads;
- *TypeIV*: components with J-leads in line.

The considered electronic types of components differ in size, number and type of pin, and geometry of the joint (see Figure 1). Electronic devices, and the materials they are made of, may be subject to life cycle loads during operating and non-operating situations. The degradation of a product (material, component, or device) depends upon the combination of different factors but, above all, the severity of the loads, that is the stress in terms of magnitude and duration of exposure. However, due to the high level of technology, mostly in electronics, the failure of a product occurs after a long time when the normal operating conditions, in terms of stress, are applied. So, in order to induce the degradation process in a short time, accelerated stress (e.g. temperature) is applied through laboratory tests. More specifically, we selected the temperature since this physical quantity is particularly important for electronic devices and components, Xu et al. (2005), Miremadi et al. (2009), and Ahmad et al. (2009).

Fig. 1: Component types representation

The stress profile was characterized by Tmax (maximum temperature) equal to $100°C$, and Tmin (minimum temperature) equal to $0°C$ with a thermal rate of $15°C/min$, a dwell time at the maximum temperature for a minimum of 10 minutes, in accordance with IPC-SM-785 (1992), as also presented in Berni et al. (2016).

Failure mechanisms work concurrently but the causes can be differentiated. Thermal aging and thermomechanical fatigue were counted as the most insidious failure mechanisms for solder degradation, these naturally happen under environmental stress and grow with strain, temperature and time. In our research both failure mechanisms, the thermal aging related to the interface finish-soldering, and the fatigue associated to the package and pin type respectively, were appraised. In order to monitor the behavior of the tested specimens, the traditional method to monitor solder joint reliability based on the measurement of Direct Current (DC) resistance was used; it can detect both soft and hard failures, and it is well suited for describing the electrical continuity. The measurement of the electrical resistance was carried out at the beginning of the test, before starting the set of thermal cycles (denoted as initial measurements or reference measurements), in order to verify the correct functionality of components and, at the same time, to assume such values as a reference for measurements obtained at the end of each thermal cycle of the test. Intermediate measurements of the electrical resistance were made at the end of each cycle in order to check the functionality or otherwise of the device being tested. On the basis of this approach, three thermal cycles were considered in our experimentation with time intervals equal to 720, 2160, and 3600 hours (30, 90, 150 days), respectively. Following, the measurement was repeated at the end of each cycle, named as time 1, time 2 and time 3. After the thermal stress cycles, a component that showed a change in the resistance value equal to, or greater than, 10% compared to the reference measure acquired before starting the tests, was considered faulty. We also considered four batches: SnPb-HASL (batch 1), SAC305- ENIG (batch 2), SAC305-I-Sn (batch 3), and

Tab. 1: Distribution of faults by batch, and by Time

Batch	**Alloy-finish**	*Time* **1**	*Time* **2**	*Time* **3**
Batch 1	SnPb-HASL	12	15	18
Batch 2	SAC305-ENIG	8	8	8
Batch 3	SAC305-I-Sn	11	11	11
Batch 4	SAC305-OSP	8	9	9

SAC305-OSP (batch 4). The entire dataset was composed of N=11568 observations; nevertheless, the size of the observations varies from 8 to 168 for each combination of "alloy-surface finish-type". In order to better analyze the reliability data, we used the mean value for each combination "alloy-surface finish-type". Therefore, 32 observations for each alloy-finish combination were available, e.g. 8 for each *Type* within a batch; the final dataset consists of N=128 observations. In Table 1, by representing the end of each cycle with the notation (*Time*), we can observe the distribution of faults by *Time*; the total number of faults is equal to 46 at time 3 (third cycle). In particular (Table 1) batch 2, relating to SAC305 as soldering alloy, is less faulty and shows defects within the first 720 hours; therefore, the components that exceed this test period seem to withstand the entire test.

Moreover, Table 2 illustrates the distribution of faults by batch and component type at time 3. *TypeI* and *TypeII* demonstrate a comparable failure behavior in all the four batches, with the occurrence of several failures. *TypeIII* shows an optimal performance without failures when considering batches 1,2,4, and with only one failure in batch 3. Type IV differs in each batch, from zero failures in batch 2 to five in batch 1.

Tab. 2: Distribution of faults by batch, by component type at time 3

Batch	**Alloy-finish**	**Component Type**	**no.faults**
Batch 1	SnPb-HASL	*TypeI*	6
		TypeII	7
		TypeIII	0
		TypeIV	5
Batch 2	SAC305-ENIG	*TypeI*	4
		TypeII	4
		TypeIII	0
		TypeIV	0
Batch 3	SAC305-I-Sn	*TypeI*	4
		TypeII	4
		TypeIII	1
		TypeIV	2
Batch 4	SAC305-OSP	*TypeI*	4
		TypeII	3
		TypeIII	0
		TypeIV	2

3. OUTLINED THEORY

In order to address the aims of the research described above, in this section we focus on the theory relating to the Weibull distribution, McCool (2012), and statistical models applied, Cox and Oakes (1984) and Zacks (2011). A detailed description of concepts and definitions relating to reliability data and statistical models can also be found in Allison (2010).

3.1 RELIABILITY: KEY CONCEPTS AND MODELING SPECIFICATIONS

In line with the aim of this study (e.g. the relevance of surface finishes for soldering reliability), the DC resistance measurements collected during the accelerated thermal life tests for each component (Section 2) are analyzed through a statistical modeling approach involving Weibull statistical models.

Let us consider N statistical units (i=1,..N); $f_i(t_i)$ is the probability density function (p.d.f.) for each unit i-*th* at time t_i. Moreover, we consider the reliability function $R(t_i) = (1 - F(t_i)) = Pr(T > t_i)$ calculated at time t_i, where $F(t_i)$ is the cumulative distribution function of failures for each i unit, and T denotes the time random variable. $R(t_i)$ is the probability that the life of i-th component (unit) will be greater than t_i. The last definition relates to the hazard function, or hazard rate, $h(t_i)$, e.g. the risk of failure for component i at time t_i. The aim of the hazard function is to quantify the instantaneous risk that an undesired event (the failure) will occur at time t_i. Because time is continuous, the probability that an event will occur at exactly time t_i is necessarily null. However, we can evaluate the probability that such an undesired event occurs in the interval between t_i and $t_i + \Delta t$, assuming that the component is failure free at time t_i. In other words, we are interested in the fact that this probability is conditional to the component surviving to time t_i. Moreover, we only want to consider those components that have experienced the event (fault) at the beginning of the interval $[t_i + \Delta t)$. Therefore, the hazard function may be expressed as follows:

$$h(t_i) = \lim_{\Delta t \to 0} \frac{F(t_i + \Delta t) - F(t_i)}{Pr\{T > t_i\}\Delta t} = \frac{f(t_i)}{R(t_i)} \tag{1}$$

When considering reliability data, the nature of the situation, e.g. censored or truncated data, must be taken into account. In this study we dealt with right censored data, i.e. all the components start at the same instant of time t_0 and if a component does not present a failure during any of the lifetime cycles, then it is a right censored unit, because we do not know what happens to this unit after completion of the follow-up period.

Two common types of right censored data exist, i.e. Type I and Type II, related to time censored and failure censored, respectively, Allison (2010). By considering right censored data, we have to divide the dataset by u uncensored and $(N-u)$ censored observations. Moreover, a dummy variable δ is specified for each statistical unit, e.g. $\delta = 0$ if the unit is censored and $\delta = 1$ if observed. Given these two sets of data, censored and uncensored, and by assuming that all the observations are independent, the likelihood function becomes:

$$L = \prod_{i=1}^{N} [f_i(t_i)]^{\delta_i} [R_i(t_i)]^{1-\delta_i} \tag{2}$$

In formula (2) the likelihood function is expressed as the product of two terms: i) the first term is related to the uncensored units; ii) the second one is related to the censored units.

Following we consider the specific distribution for reliability data, according to formula (2). In the application (Section 4), we assume that data are distributed according to a Weibull distribution, and Weibull random-effects models are applied, also for evaluating the probabilities for failure times. Furthermore, the two-parameter Weibull distribution has the following p.d.f.:

$$f_W(t) = \gamma\alpha(\alpha t)^{\gamma-1} \exp(-(\alpha t)^{\gamma}) \tag{3}$$

$$\alpha = \exp(-x'\beta) \tag{4}$$

where $\gamma \in (0,\infty)$ is the Weibull shape parameter, t is the time variable, x is the vector of covariates and β is the column vector relating to the unknown coefficients. The γ coefficient is also interpreted as a failure rate: $\gamma \in (0,1)$ implies a monotonic decreasing of the failure rate, while $\gamma > 1$ means that the failure rate monotonically increases over time. An additional parameter is the scale parameter ($\hat{\sigma} = 1/\gamma$), which describes the shape of the Weibull distribution, and also allows us to interchange between survival and proportional hazard analyses. This means that Weibull estimated coefficients, when transformed, can be interpreted as relative hazard ratios. In fact, the Weibull model as well as the Exponential model, which is a special case of the former, is the only model that simultaneously belongs to both these model types.

The Weibull reliability and hazard functions may be expressed as follows:

$$R_W(t) = exp\{-(\alpha t)^{\gamma}\} \tag{5}$$

$$h_W(t) = \gamma\alpha(\alpha t)^{\gamma-1} \tag{6}$$

The specific modeling approach is carried out by considering a two-by-two comparison of surface finishes. The corner-point parametrization allows for better performing this comparative study. Therefore, the built dummy variable allows for using the traditional alloy-finish combination as a reference level, and for evaluating the difference between the two surface finishes. Furthermore, for each comparison, α (formula (4)) is specifically defined for the $i-th$ unit as

$$\alpha_i = \exp\Big(-\beta_0 - \sum_{j=1}^{2} \beta_{S_j} x_{iS_j} - \sum_{l=1}^{4} \beta_{T_l} x_{iT_l}\Big) \tag{7}$$

where S_j for $j = 1,2$ denotes the two surface finishes compared, and T_l for $l = 1,..,4$ are coefficient suffixes relating to the four types, e.g. $TypeI - TypeIV$, of the electronic components (Figure 1, Section 2). Moreover, for all the comparisons, we normalized for each component type by dividing the electrical resistance values by the pin size. Thus, the binary response variable (failure, non-failure) takes care of the pin size normalization through the standardized resistance values.

The estimated results are obtained through the Accelerate Failure Time (AFT) approach, which is a quantitative measure of the lifetime (accelerated lifetime analysis) for a generic component. Therefore, a positive coefficient β_{AFT} implies an improvement of the lifetime for the statistical unit, e.g. the alloy-finish-type combination. Nevertheless, the same result could also be viewed and measured by the Proportional Hazard (PH) parametrization through the following expressions:

$$\begin{aligned} \beta_{PH} = -(\gamma\beta_{AFT}) = -\left(\frac{\beta_{AFT}}{\hat{\sigma}}\right) \\ HR = \exp(\beta_{PH}) \end{aligned} \tag{8}$$

where HR denotes the Hazard Ratio, and $\hat{\sigma}$ is the scale parameter. In the case study, as reported in detail in Section 2, the final dataset consists of $N = 128$ observations, see Table 2. Failure is defined as a 10% variation in the response variable (Y) after each cycle lifetime.

The next section illustrates the estimation results of the models and coefficients defining the Weibull distribution. The statistical results are obtained through the NLMIXED procedure (SAS software, Windows platform, version 9.2).

4. MODEL RESULTS

The two-by-two comparisons of the surface finishes are the following:

Tab. 3: Model estimates of SnPb-HASL *versus* SAC305-OSP

Coefficient	**Est.**	**Std. err.**	**Pr** $> \|t\|$
β_0	4.4820	0.3326	<0.0001
β_{S_1}	0	.	.
β_{S_2}	0.9186	0.4149	0.0304
β_{T_1}	0	.	.
β_{T_2}	0.1128	0.4342	0.7959
β_{T_4}	0.5806	0.4851	0.2358
γ	1.0302	0.1703	<0.0001

1. the traditional SnPb-HASL alloy-finish combination *versus* the SAC305-OSP alloy-finish combination (Section 4.1);
2. the SAC305-ENIG in comparison with the SAC305-OSP alloy-finish combination (Section 4.2);
3. the SAC305-I-Sn *versus* the SAC305-OSP alloy-finish combination (Section 4.3).

Model fitting and estimates are checked by also evaluating the AIC (Akaike Information Criterion) index, the Log-Likelihood value, and additional convergency information, e.g. the number of iterations and the maximum absolute gradient element.

4.1 FIRST RELIABILITY COMPARISON: SNPB-HASL VERSUS SAC305-OSP

The first comparison involves the SnPb-HASL surface finish versus the SAC305-OSP surface finish. The model results are shown in Table 3. In this first comparison, only three types of components ($TypeI, TypeII, TypeIV$) are analyzed; in fact, failures were not observed when considering the third type of component ($TypeIII$). Thus in this case $\beta_{T_l}; l = 1,2,4$ are the three estimated coefficients for the component types: I, II, IV, respectively. The estimated coefficients β_{S_1} and β_{S_2} relate to SnPb-HASL and SAC305-OSP, respectively. Thus, the performance reliability of SAC305-OSP is evaluated *versus* the SnPb-HASL, e.g. the reference level. We can observe that the estimate $\beta_{S_2} = 0.9186$ means that the lifetime of SAC305-OSP is higher than the SnPb-HASL lifetime, even though it is lower than one. This result implies a decrease in the failure risk with a hazard ratio (HR) equal to 0.39, see formula (8), and an estimated lower failure risk for the SAC305-OSP alloy-finish combination with respect to the SnPb-HASL.

By considering the influence of the component types in the model estimation, we can observe how both the estimated coefficients, for $TypeII$ and $TypeIV$, are positive ($\beta_{T_2} = 0.1128$, $\beta_{T_4} = 0.5806$) with respect to the reference type ($TypeI$); however, neither coefficient show significant p-values, even though $TypeIV$ shows a not negligible p-value. These results mean that an increase in the lifetime of the circuit board is observed when these types are applied with respect to the reference type ($TypeI$). In addition, the hazard ratio, equal to 0.55 for $TypeIV$, confirms this. Moreover, it must be noted that a failure for a single type of electronic component implies a failure for the whole electronic device.

The estimate of γ coefficient is highly significant and is greater than one; this result confirms that the failure risk monotonically increases over time. Finally, the estimated coefficient β_0 is highly significant. This result corresponds to the basic risk level for the alloy-finish (SnPb-HASL) with $TypeI$ component. Nevertheless, by considering formula (8), the proportional hazard coefficient is equal to $exp(-4.5353) = 0.0098$, which is the baseline risk. Figure 2 shows the cumulative distribution functions for each surface finish per $Type$; the dashed lines refer to the SnPb-HASL alloy-finish combination, and show the failure probability within time t per $Type$; the solid lines refer to the SAC305-OSP alloy-finish. We can observe how the failure probability at time t (days), $t \in [0;150]$, is higher for the surface finish assumed as the reference level. In Figure 3, where the Kaplan-

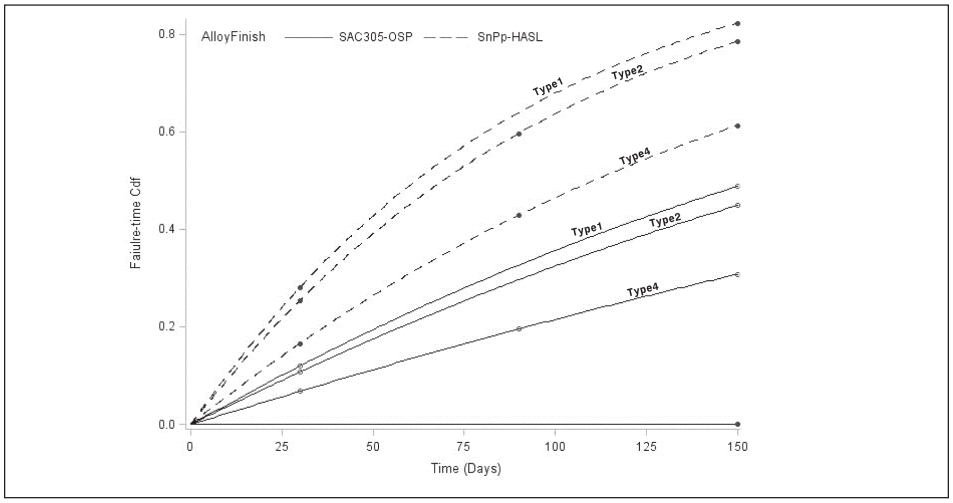

Fig. 2: Cumulative distribution functions for SnPb-HASL and SAC305- OSP combinations of alloy-finish per *Type*

Meier curves are illustrated, we observe that the solid line (SAC305-OSP alloy-finish) always shows a higher reliability function than the same curve calculated for the SnPb-HASL alloy-finish (dashed line).

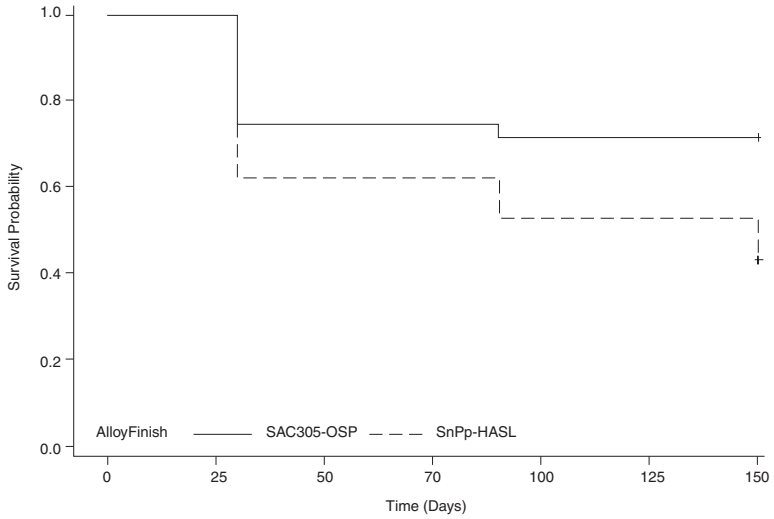

Fig. 3: Kaplan-Meier curves: SnPb-HASL vs. SAC305-OSP

Tab. 4: Model estimates for SAC305-ENIG *versus* SAC305-OSP

Coefficient	**Est.**	**Std. err.**	**Pr** $> \|t\|$
β_0	5.3703	0.5691	<0.0001
β_{S_1}	0	.	.
β_{S_2}	-0.1008	0.6121	0.8696
β_{T_1}	0	.	.
β_{T_2}	0.2569	0.6521	0.6949
β_{T_4}	2.2160	1.0787	0.0440
γ	0.7956	0.1737	<0.0001

4.2 SECOND RELIABILITY COMPARISON: SAC305-ENIG *VERSUS* SAC305-OSP

The second subsection analyzes the SAC305-ENIG surface finish in comparison with the SAC305-OSP finish. Table 4 shows the model results; also in this case, the *TypeIII* component does not show any faults. By observing the estimated coefficients β_{S_1} and β_{S_2}, we can see how the SAC305-OSP finish shows a negative estimate ($\beta_{S_2} = -0.1008$) *versus* the SAC305-ENIG finish, e.g. the reference level. This result means that the SAC305-OSP finish shows lower relia-

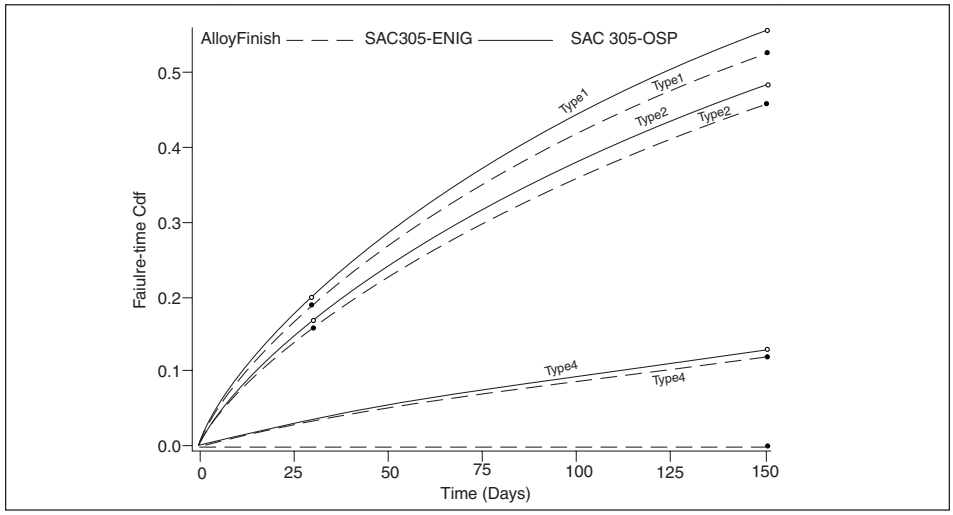

Fig. 4: Cumulative distribution functions for SAC305-ENIG and SAC305- OSP alloy-finish combinations per *Type*

bility, or a lower lifetime probability; similarly, it can be interpreted as being at a greater risk of fault when compared with the SAC305-ENIG. The hazard ratio is equal to 0.9229, which confirms the major risk of fault for the OSP surface finish. Nevertheless, the coefficient β_{S_2} does not show a significant p-value for this finish, highlighting that the SAC305-OSP shows a very similar behavior compared with the SAC305-ENIG, and a lower difference when considering the first two-by-two comparison, e.g. SnPb-HASL *versus* SAC305-OSP, (Section 4.1).

Regarding the *Type* variable, *TypeII* shows a positive coefficient 0.2569, which means greater reliability with respect to *TypeI*, even though with a negligible p-value. On the contrary, when considering *TypeIV*, this component shows greater reliability in comparison with *TypeI*; in fact, the estimated coefficient 2.2160, which is significant at 5% level, is greater than one, with HR equal to 0.1715.

The coefficient γ is highly significant and is notably lower than one; this means that over time the number of failures show a decline. The estimated coefficient β_0 is highly significant, and it is the basic level of risk for the reference levels formed by the SAC305-ENIG surface finish and *TypeI* component. The baseline risk is equal to $exp(-4.2726) = 0.0139$. Figure 4 shows the cumulative distribution functions calculated for each alloy-finish combination per component *Type*. Undoubtedly, an improvement can be observed in the SAC305-OSP lifetime (solid

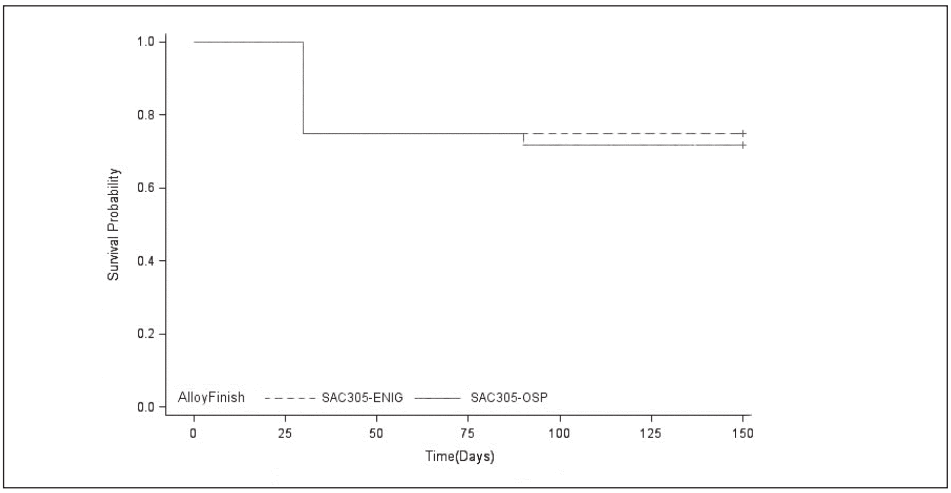

Fig. 5: Kaplan-Meier curves: SAC305-ENIG versus SAC305-OSP

line). When considering the Kaplan-Meier curves (Figure 5) the distance between the solid line (SAC305-OSP alloy-finish), and the dashed line (SAC305-ENIG) is not as relevant, and is lower than the distance observed in Figure 3 between the SnPb-HASL and SAC305-OSP alloy-finishes. However, the SAC305-OSP alloy-finish shows the worst reliability function with much lower probabilities at the end of the lifetime cycle.

4.3 THIRD RELIABILITY COMPARISON: SAC305-I-SN VERSUS SAC305-OSP

The final comparison analyzes the SAC305-I-Sn surface finish versus the SAC305-OSP finish. Table 5 contains the model results; it must be noted that in this case, all the components, e.g. also the *TypeIII*, show failures (Table 2). Considering the estimated coefficients β_{S_1} and β_{S_2}, we can see how the SAC305-OSP finish demonstrates a positive estimate ($\beta_{S_2} = 0.3361$) with respect to the finish used as the reference, e.g. the SAC305-I-Sn. This result means that the SAC305-OSP finish shows greater reliability, or greater lifetime probability; similarly, it can be interpreted as a lower risk of fault when compared with the SAC305-I-Sn. The hazard ratio is equal to 0.7690, which confirms the major risk of failure for the I-Sn surface finish. Nevertheless, the coefficient β_{S_2} does not show a significant p-value, pointing out that also for these two finishes the performance is very similar, and it is worse when compared with the first two-by-two comparison, e.g. the SAC305-OSP *versus* the SnPb-HASL finish, Section 4.1.

When considering the *Type* variable, all the estimated coefficients are pos-

Tab. 5: Model estimates for SAC305-I-Sn *versus* SAC305-OSP

Coefficient	Est.	Std. err.	Pr $>\|t\|$
β_0	5.1739	0.5286	<0.0001
β_{S_1}	0	.	.
β_{S_2}	0.3361	0.5784	0.5632
β_{T_1}	0	.	.
β_{T_2}	0.2461	0.6637	0.7120
β_{T_3}	3.1616	1.4748	0.0359
β_{T_4}	1.2339	0.8099	0.1326
γ	0.7814	0.1586	<0.0001

itive; this means that all the *Types II*,*III*,*IV* are better than the *TypeI*, e.g. the reference Type. Nevertheless, it must be noted that two components (e.g. *TypeIII* and *TypeIV*) show a significant or a relevant p-value; while *TypeII* shows a positive coefficient 0.2461, and a greater reliability with respect to *TypeI*, but with a negligible p-value. Conversely, when considering *TypeIII*, this type shows greater reliability in comparison with *TypeI*, in fact the estimated coefficient 3.1616, which is significant at 5% level, is notably greater than one, with HR equal to 0.0845. Finally, the estimated coefficient obtained for *TypeIV*, and equal to 1.2339, shows a not negligible p-value by confirming an improvement of this component with respect to *TypeI*; the calculated HR is equal to 0.3813.

The coefficient γ is highly significant and is notably lower than one, therefore there is a decrease in the number of faults over time. The estimated coefficient β_0 is highly significant. It is the basic level of risk for the reference levels of surface finish (SAC305-I-Sn) and *TypeI* component. The baseline risk, calculated through formula (8), is equal to $exp(-4.0429) = 0.0175$. Both Figures (Figure 6 and 7) confirm the model results; the cumulative distribution function per *Type*, depicted in Figure 6, shows that *Type* and SAC305-I-Sn (dashed line) are always above the solid lines, corresponding to SAC305-OSP and *Type*. Figure 7, related to the Kaplan-Meyer curve, points out the best behaviour of the SAC305-OSP alloy-finish combination for the whole interval of the thermal cycle.

5. DISCUSSION AND FINAL REMARKS

The research activity presented aims at evaluating the reliability performance of electronic boards, with a focus on solder joints. Circuit boards with compo-

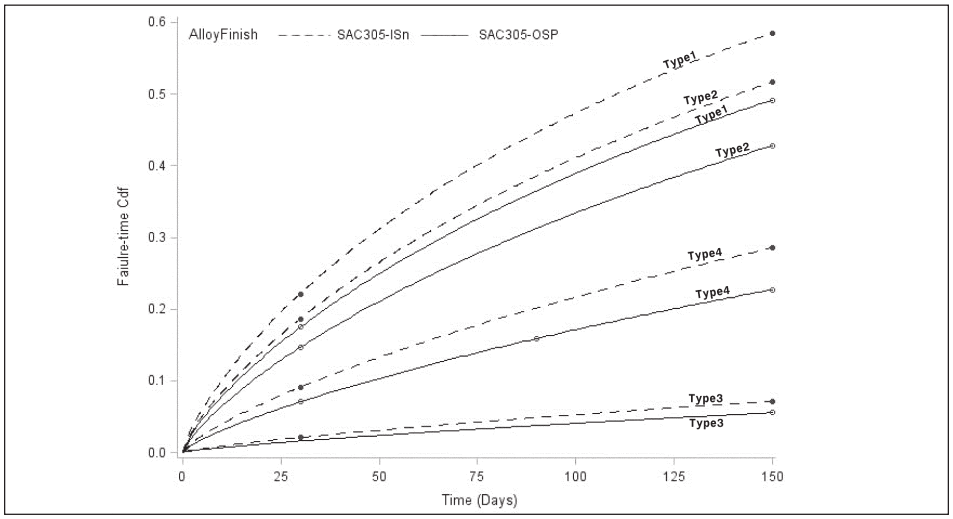

Fig. 6: Cumulative distribution functions for SAC305-I-Sn and SAC305- OSP alloy-finish combinations per *Type*

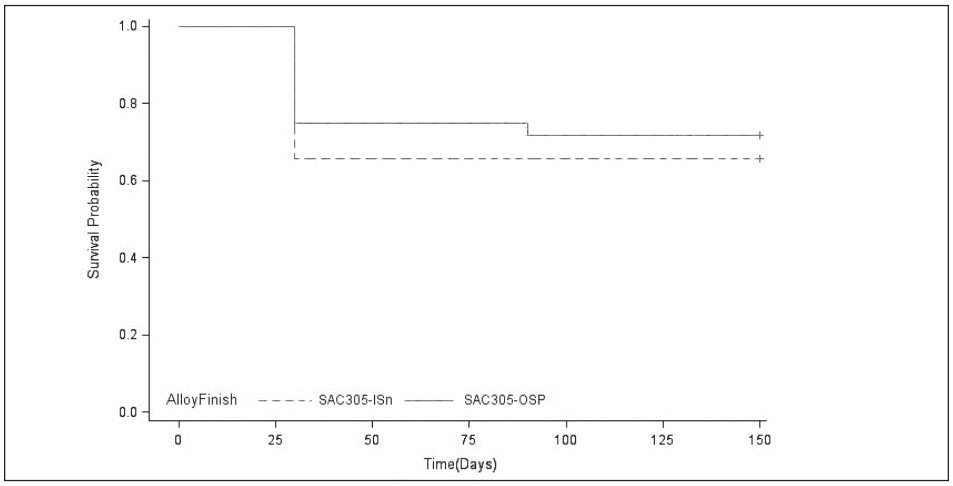

Fig. 7: Kaplan-Meier curves: SAC305-I-Sn versus SAC305-OSP

nents soldered with lead-tin and SAC305 soldering alloys were evaluated. Different surface finishes of the boards were considered, and their combination with the alloy was reported. Three two-by-two comparisons were carried out; e.g. the SAC305-OSP was compared with the traditional SnPb-HASL combination (Section 4.1), and with SAC305-ENIG (Section 4.2); the last comparison relates to

SAC305-I-Sn and SAC305-OSP (Section 4.3). The statistical analysis was performed through the application of Weibull models. By evaluating the statistical results obtained, the SAC305, with ENIG finish, demonstrated greater reliability with respect to the boards soldered, except when involving the SAC305-OSP combination. On the contrary, the OSP surface finish presented a better performance in comparison with the traditional SnPb-HASL. The same behavior has been observed in the final comparison, where the SAC305-OSP combination showed a lower probability of failures with respect to the SAC305-I-Sn. In fact, the first comparison, e.g. the traditional combination *versus* SAC305-OSP, achieved a value of the hazard ratio that revealed greater reliability, showing a significant reduction in the failure risk. In the second comparison, e.g. SAC305-ENIG *versus* SAC305-OSP, the estimated coefficient linked to the surface finish appeared negligible and, above all, it resulted negative, showing a lower reliability gap.

Therefore, in this case, the SAC305-OSP alloy-finish combination showed slight unreliability with respect to the ENIG finish.

As regards the type of components, it is interesting to emphasize how *TypeIII* did not show any failures during the accelerated thermal test in batch 1, 2 and 4; the *TypeIV* gave rise to a significant increase in life duration of batch 2.

The final comparison showed an improvement in reliability when the SAC305-OSP combination has been used; in this case, all the Types showed failures, nevertheless *TypeIII* resulted in being the best type of component among all the Types, assuming *TypeI* as the reference level.

In all the comparisons, the Weibull shape parameter (γ) resulted highly significant: i) in Table 3 it was slightly greater than one, e.g. the faults resulted uniformly distributed over time; ii) in Tables 4 and 5 it was lower than one, showing a decreasing of failures over time.

To conclude, it should be pointed out that in general, the SMT and gull wing (*TypeIII*) components demonstrated the most reliable behavior with all the soldering materials. *TypeIV*, characterized by plastic package and pin in line (see Figure 1), seemed to be the second most reliable component, and it achieved a very good performance in conjunction with the ENIG finish. It is also important to underscore that within batches the least reliable behavior was identified for *TypeI* and *TypeII*, e.g. the surface mount components without pins and with ball grid array respectively.

Moreover, in all the three comparisons, the estimated coefficients for *TypeII* were always non-significant and also negligible with respect to *TypeI*, highlighting a similar behavior observed for these two component types.

Furthermore, it must be noted that this study provides relevant information about the new soldering technology: the best reliability performers among the surface finishes has been obtained by ENIG and OSP, for which a very small difference was observed. Therefore, we can conclude that in electronics the OSP finish could be a cheaper alternative to the ENIG finish because it was able to meet comparable technical and reliability requirements, as well as being environment-friendly.

REFERENCES

Ahmad, M., Xie, W., Liu, K. C., Xue, J., Towne, D. (2009). Parametric acceleration transforms for Lead-free solder joint reliability under thermal cycling conditions. *Proceedings IEEE Electronic Components and Technology Conf. (ECTC)*, San Diego, CA, USA, pp. 682-691.

AIM, (2007). *Lead Free Soldering Guide Alloys, Chemistries, Data, Training, Consultation*. AIM Manufacturing and Distribution Worldwide.

Allison, P.D. (2010). *Survival analysis using SAS- A practical guide*, 2nd Ed., SAS Institute Inc., Cary, NC, USA.

Andersson, C., Andersson, D., Tegehall, P., Liu, J. (2004). Effect of different temperature cycle profiles on the crack propagation and microstructural evolution of Lead free solder joints of different electronic components. *Proceedings IEEE Int. Conf. Thermal, Mechanical and Multiphysics Simulation and Experiments in Micro-Electronics and Micro-Systems (EuroSIME)*, Brussels, Belgium, pp. 455-464.

Berni, R., Catelani, M., Fiesoli, C., Scarano, V.L. (2015). A Comparison of Alloy-Surface Finish Combinations Considering Different Component Package Types and Their Impact on Soldering Reliability. *IEEE Transactions on Reliability,* Vol. 65, pp. 272-281.

Bradley, E., Handwerker, C. A., Bath, J.R., Parker, D., Gedney, R. W. (2007). *Lead-free electronics*, John Wiley & Sons, Hoboken, NJ.

Catelani, M., Scarano, V.L., Berni, R. (2013). Optimization of accelerated testing through design of experiment for ageing of Lead-free electronic interconnection material. *International Journal of Metrology and Quality Engineering*, Vol. 4, pp. 47-54.

Cheng, M.D., Chang, S.Y., Yen, S.F.,Chuang, T.H. (2004). Intermetallic compounds formed during the reflow and aging of Sn–3.8 Ag–0.7 Cu and Sn20In2Ag0.5 Cu solder ball grid array packages. *Journal of Electronic Materials*, Vol. 33, 171-180.

Clech, J.P. (2007). *Lead-Free Solder Joint Reliability*, Springer, USA.

Collins, M.N., Punch, J., Coyle, R. (2012) Surface finish effect on reliability of SAC305 soldered chip resistors. *Soldering Surface Material Technology*, Vol. 24, pp. 240-248.

Cox, D.R., Oakes, D. (1984). *Analysis of Survival Data*, Chapman & Hall, Boca Raton, Florida.

Cuddalorepatta, G., Dasgupta, A. (2007). Creep and stress relaxation of hypoeu tectic Sn3.0Ag0.5Cu Pb-free alloy: Testing and modeling. *Proceedings ASME International Mechanical Engineering Congress and Exposition*, pp. 1-9.

Dudek, R., Faust, W., Ratchev, R., Roellig, M., Albrecht, H. J., Michel, B. (2008).

Thermal test- and field cycling induced degradation and its FE-based prediction for different SAC solders. *Proceedings Intersociety Conference on Thermal and Thermomechanical Phenomena in Electronic Systems,(ITHERM)*, Lake Buena Vista, FL, USA, pp. 668-675.

Hossain, M.M., Zahedi, F., Agonafer, D., Dunford, S.O., Viswanadham, P. (2006). Reliability of Lead (Pb) free SAC solder interconnects with different PWB surface finishes under mechanical loading. *Proceddings IEEE Intersociety Conference on Thermal and Thermomechanical Phenomena in Electronic Systems (ITherm)*, San Diego, CA, USA, pp. 1039-1048.

IPC-D-279(1996). *Design Guidelines for Reliable Surface Mount Technology Printed Board Assemblies*. IPC, Bannockburn, IL.

IPC/JEDEC J-STD-020C (2004) *Moisture/Reflow Sensitivity Classification for Non-hermetic Solid State Surface Mount Devices*. IPC, Bannockburn, IL.

IPC-SM-785 (1992). *Guidelines for Accelerated Reliability Testing of Surface Mount Solder Attachments*. The Institute for Interconnecting and Packaging Electronic Circuits, Northbrook, IL.

Islam, M.N., Chan Y.C. (2005). Interfacial reactions of Cu-containing lead-free solders with Au/NiP metallization. *Journal of Electronic Materials* Vol. 34, pp. 662-669.

Kim, D.H., Elenius, P., Barrett, S. (2002). Solder joint reliability and characteristics of deformation and crack growth of Sn-Ag-Cu versus eutectic Sn-Pb on a WLP in a thermal cycling test. *IEEE Transactions on Electronics Packaging Manufacturing*, Vol. 25, pp. 84-90.

Kim, S.-W., Yoon, J.-W., Jung, S-B. (2004). Interfacial reactions and shear strengths between Sn-Ag-based Pb-free solder balls and Au/EN/Cu metallization. *Journal of Electronic Materials* Vol. 33, pp. 1182-1189.

Lau, J.H. (1991). *Solder Joint Reliability: Theory and Application*, Springer Science, USA.

Lau, J.H., Pao, Y. H. (1997). *Solder joint reliability of BGA, CSP, flip chip, and fine pitch SMT assemblies*, McGraw-Hill, New-York.

Liu, Y., Sun, F., Zhang, H., Xin, T., Yuan, C.A., Zhang, G. (2015). Interfacial reaction and failure mode analysis of the solder joints for flip-chip LED on ENIG and Cu-OSP surface finishes. *Microelectronics Reliability* Vol. 55, pp. 1234-1240.

Ma, H., Suhling, J.C., Zhang, Y., Lall, P., Bozack, M.J. (2007). The influence of elevated temperature aging on reliability of Lead free solder joints. *Proceedings IEEE Electronic Components and Technology Conference (ECTC)*, Sparks, NV, USA, pp. 653-668.

McCool, J.I. (2012). *Using the Weibull distributions*, John Wiley & Sons, NJ.

Miremadi, J., Henshall, G.A., Allen, A., Benedetto, E., Roesch (2009). M. Lead-Free solder joint reliability model enhancement. *Proceedings International Symposium on Microelectronics (IMAPS)*, San Jose, CA, USA.

Osterman, M., Dasgupta, A. (2007). Life expectancies of Pb-free SAC solder interconnects in electronic hardware. *Journal of Materials Science: Materials in Electronics*, Vol. 18, pp. 229-236.

Puthota, R.(2021). *PCB vs PCBA Process Challenges & Solutions*, https: //docplayer.net/19723948-Pcb-vs-pcba-process-challenges-solutions.html, available pdf (accessed: January 8th, 2021).

Shangguan, D. (2006). Lead-Free Solder Interconnect Reliability. *ASM International*, Materials Park, Ohio.

Shunfeng C, Chien-Ming H, Michael P. (2017). A review of lead-free solders for electronics applications.*Microelectronics Reliability*, Vol.75, pp. 77-95.

Sinan S, Sa'd H, Khozima H. (2019). Effect of Surface Finish on the Shear Properties of SnAgCu-Based Solder Alloys. *IEEE Transactions On Components, Packaging And Manufacturing Technology*, Vol. 9, pp. 1473-1485.

Suganuma, K. (2001). Advances in Lead-free electronics soldering. *Current Opin- ion in Solid State & Material Science*, Vol. 5, pp.55-64.

Sun, P., Andersson, C., Wei, X., Cheng, Z., Shangguan, D., Liu, J. (2006). High temperature aging study of intermetallic compound formation of Sn" 3.5Ag and Sn" 4.0Ag" 0.5Cu solders on electroless Ni(P) metallization. *Journal of Alloys and Compounds,* Vol. 425, pp. 191-199.

Vasudevan, V., Fan, X. (2008). An acceleration model for Lead-free (SAC) solder joint reliability under thermal cycling. *Proceedings Electronic Components and Technology Conference (ECTC),* Lake Buena Vista, FL, USA, pp. 139-145.

Vianco, P.T. (2019). A Review of Interface Microstructures in Electronic Packaging Applications: Soldering Technology. *Advances in Electronic Interconnection Material*, Vol. 71, pp. 158-171.

Xia, Y., Xie, X. (2008). Reliability of lead-free solder joints with different PCB surface finishes under thermal cycling. *Journal of Alloys Compounds* Vol. 454, pp. 174-179.

Xu, L., Pang, J.H.L., Prakash, K.H., Low, T.H. (2005). Isothermal and thermal cycling aging on IMC growth rate in Lead-free and Lead-based solder interface. *IEEE Transactions On Components and Packaging Technology*, Vol. 28, pp. 408-414.

Yu, S.Y., Kwon, Y.M., Kim, J., Jeong, T., Choi, S., Paik, K.W. (2012). Studies on the Thermal Cycling Reliability of BGA System-in-Package (SiP) With an Embedded Die. *IEEE Transactions on Packaging Manufacturing Technology,* Vol. 2, pp. 625-633.

Zacks S. (2011). *Introduction to reliability analysis*, Springer-Verlag, New York.

Zhang, Y., Cai, Z., Suhling, J.C., Lall, P., Bozack, M.J. (2008). The effects of aging temperature on SAC solder joint material behavior and reliability. *Proceedings IEEE Electronic Components and Technology Conference (ECTC)*, Lake Buena Vista, FL, USA, pp. 99-112.

Zribi, A., Clark, A., Zavalij, L., Borgesen, P., Cotts, E.J. (2001). The growth of intermetallic compounds at Sn-Ag-Cu solder/Cu and Sn-Ag-Cu solder/Ni interfaces and the associated evolution of the solder microstructure. *Journal of Electronic Materials,* Vol. 30, pp. 1157-1164.